Available online at www.sciencedirect.com
ScienceDirect
Journal of Hazardous Materials 150 (2008) 153–157
Journal of Hazardous Materials
www.elsevier.com/locate/jhazmat

Sonochemical synthesis and photocatalytic activity of meso- and macro-porous TiO_2 for oxidation of toluene

Yang Liu [a,b], Yan Li [a], YuntaoWang [a], Lei Xie [a], Jie Zheng [a], Xingguo Li [a,*]

[a] *Beijing National Laboratory for Molecular Sciences (BNLMS) (The State Key Laboratory of Rare Earth Materials Chemistry and Applications), College of Chemistry and Molecular Engineering, Peking University, Beijing 100871, China*

[b] *Beijing Key Laboratory of Bioactive Substances and Functional Foods, College of Arts and Science, Beijing Union University, Beijing 100083, China*

Received 4 November 2006; received in revised form 11 April 2007; accepted 19 April 2007
Available online 24 April 2007

Abstract

Meso-and macro-porous TiO_2 were synthesized by ultrasonic induced solvothermal method. Octadecylamine as a soft template was used to direct the formation of porous structure. The as-prepared porous TiO_2 was characterized by low angle and wide angle X-ray diffraction, N_2 adsorption–desorption isotherms and BET surface area. The energy influence of ultrasound and heat and concentration of nitric acid for post extraction on formation of porous structure were investigated. The photocatalytic activities of TiO_2 were investigated by degrading toluene gas under UV light. The results revealed that proper energy facilitates the formation of porous structure and too low concentration of nitric acid cannot extract template from pores. The photocatalytic activities of TiO_2 with porous structure are higher than those of nonporous ones.

Keywords: Photocatalysis; Mesoporous; Macroporous; Titanium dioxide; Toluene

1. Introduction

Indoor air pollution has been a serious problem in many developing countries. Volatile organic compounds (VOCs) as indoor air pollutants are threatening the health of humans. Toluene is one of the aromatic VOCs, which is from perfume, detergent, painting, wallpaper, bond, cigarettes and so on. Human exposure to toluene for a long time can lead to damage to the nervous system. Therefore, degradation of toluene in the air is receiving comprehensive attention. To date, TiO_2 is widely used as a photocatalyst because of its remarkable photocatalytic activity and stability, besides its application in the new generation of solar cells, electrochromic devices and self-cleaning devices. Especially, TiO_2 photocatalyst is used to remove environmental contaminants. In the last ten years, TiO_2 with its mesoporous structure has been of particular interest because of its high specific surface area, which leads to its notable performance in degrading toxic organic compounds in air and water. Mesoporous TiO_2 with high specific surface area can provide more active sites to adsorb reactant molecules and facilitate accessibility of reactants to the catalysts. Light efficiency is enhanced due to the enlarged specific surface area and multiple scattering [1].

Mesoporous TiO_2 was generally prepared through hydrothermal methods based on the ordered micelle of surfactants, such as alkyl bromide [2], alkyl phosphate [3], long-chain amine [4], block copolymer [5], and so on. However, it is difficult to maintain the mesoporous structure after calcinations and obtain a crystalline framework because the removal of templates may lead to the collapse of the mesoporous structure. In this study, we used alkylamine as the template to synthesize porous TiO_2 induced by ultrasound and used nitric acid to extract the soft templates for the formation of mesopores. The influence of energy provided by ultrasound and heat and concentration of nitric acid

* Corresponding author. Tel.: +86 10 6276 5930; fax: +86 10 6276 5930.
E-mail address: xgli@pku.edu.cn (X. Li).

0304-3894/$ – see front matter © 2007 Published by Elsevier B.V.
doi:10.1016/j.jhazmat.2007.04.088

on the formation of pores is explored. The photocatalytic activities of as-prepared TiO_2 for oxidation of toluene were also investigated.

2. Experimental

2.1. Synthesis

Porous TiO_2 samples were synthesized by solvothermal condensation of tetrabutyltitanate with octadecylamine as surfactant template. 3.4 ml $Ti(OC_4H_9)_4$ (0.01 mmol) and 0.9 g octadecylamine (0.003 mmol) were dissolved in 10 ml absolute ethanol under stirring, respectively. Then the alcohol solution of tetrabutytitanate was dropped into the solution of surfactant template under magnetic stirring. The mixture was stirred for 60 min to obtain a transparent solution. Twenty milliliters of distilled water were added dropwise into the resulting solution under stirring. The resulting suspension contained in 50 ml round bottom flask was sonicated by ultrasound with different intensity for 6 h. TiO_2-1 and TiO_2-2 were sonicated with 50 W cm^{-2} intensity of ultrasound (KQ-100B, 40 kHz), aged at 333 K. The difference of preparation between TiO_2-1 and TiO_2-2 was the adding order of distilled water. The mixture of the solution of template and inorganic precursor was added into the distilled water during TiO_2-2 synthesis. TiO_2-3, TiO_2-4, TiO_2-5 and TiO_2-6 solutions were sonicated by ultrasonic probe (titanium horn, Ø3, 0.24 cm diameter, 40 kHz), aged at 298 K. The ultrasonic intensity for TiO_2-3 was 100 W cm^{-2}, and that for TiO_2-4, TiO_2-5 and TiO_2-6 were 250 W cm^{-2}. Then, the white precipitate was separated by centrifugation. In order to remove the surfactant template, the samples were treated with nitric acid of different concentrations for a few minutes. Then, the precipitate was washed with absolute ethanol and dried under vacuum at 323 K overnight, then calcined in air at 673 K for four hours. The main conditions of synthesis were summarized in Table 1.

2.2. Characterization

Wide-angle and low-angle X-ray diffraction experiments were carried out on a Rigaku D/ MAX 200 X-ray powder diffractometer using Cu Kα radiation. Specific surface areas (BET), Barrett–Joyner–Halenda (BJH) pore size distribution and pore parameters of the powder samples were determined by nitrogen adsorption–desorption isotherm measurements at 77 K using a SA3100 Plus (Beckman Coulter, USA) apparatus. All samples were outgased at 473 K for 40 min before the analysis.

2.3. Photocatalytic activity

The as-received TiO_2 samples were used as photocatalyst to degrade toluene. The photocatalytic reaction was performed in a quartz reactor (250 ml) irradiated by a high-pressure mercury lamp (250 W, center wavelength is 365 nm) located at a fixed distance 25 cm from the reactor. The rate of toluene degradation was measured by gas chromatography (GC-14CPTF, Shimadzu) equipped with a FID detector and a CBP10-M25-025 capillary column. The injection chamber temperature, column temperature and detector temperature of gas chromotography are 423, 323 and 423 K, respectively.

After 0.01 g TiO_2 was put into the quartz reactor, the system was evacuated. 0.2 μl liquid toluene and 50 ml oxygen were injected into the reactor, respectively. Nitrogen was charged into the reactor until the pressure reached 1.0×10^5 Pa. Before the high-pressure mercury lamp was turned on, the reactor was kept in dark for 120 min in order to ensure the adsorption equilibrium of toluene on the gas–solid interface. The concentration of toluene versus time was measured by GC.

3. Results and discussion

3.1. XRD

Fig. 1 shows the results of wide angle XRD, which indicates that TiO_2-1, TiO_2-2, TiO_2-3 are all anatase, and TiO_2-4, TiO_2-5 and TiO_2-6 are poorly crystallized. The corresponding particle sizes are calculated according to the Scherrer equation, and summarized in Table 1. The size of TiO_2 particles is typically in the range from 5 to 9 nm. The results of low-angle XRD measurements are shown in Fig. 2. There is a diffraction peak at 1.06° for TiO_2-1, 1.30° for TiO_2-4, 0.82° for TiO_2-5, respectively. The peaks at the lower angle suggest the existence of a large lattice plane distance (*D* value), corresponding to the ordered mesoporous structure. As only one peak is observed in the low-angle range, the mesoporous structure of TiO_2 is typically of long-range order in nature [6]. Low-angle XRD patterns of TiO_2-2, TiO_2-3 and TiO_2-6 show no diffraction peak, indicating no mesoporous structure in the samples [7].

TiO_2-1 has a porous structure, while TiO_2-2 does not. TiO_2-1 and TiO_2-2 were prepared under the same ultrasonic conditions

Table 1
Specific surface area, pore parameters derived from N_2 adsorption data, crystal size and D spacing data, photocatalytic reaction rate constant

Sample	Ultrasound intensity (W cm^{-2})	Aged temperature (K)	Concentration of nitric acid (mol l^{-1})	*D* spacing (nm)	Crystal size (nm)	Specific surface area (m^2 g^{-1})	Rate constant of photocatalytic reaction (μmol l^{-1} min^{-1})
TiO_2-1	50	333	0.15	8.3	5.4	93.09	0.0150
TiO_2-2	50	333	0.15	–	6.2	110.39	0.0225
TiO_2-3	100	298	0.15	–	8.8	47.59	0.0163
TiO_2-4	250	298	0.15	6.8	–	289.45	0.0219
TiO_2-5	250	298	1.5	10.8	–	317.94	0.0322
TiO_2-6	250	298	0.015	–	–	17.91	0.0118

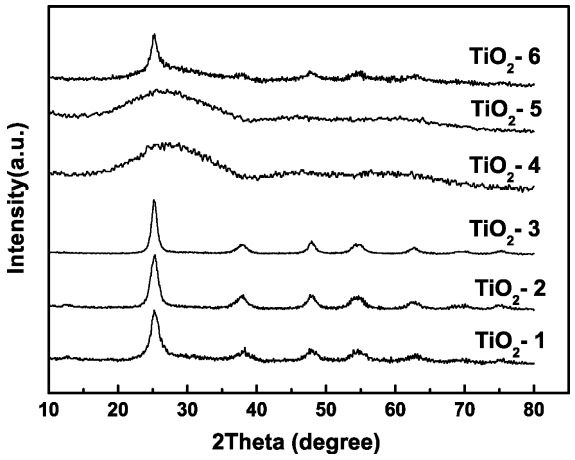

Fig. 1. Wide-angle XRD pattern of TiO_2 calcined at 673 K for 4 h.

and at the same aging temperature. For TiO_2-2, ethanol solution of $Ti(OC_4H_9)_4$ was added into distilled water. The hydrolysis of $Ti(OC_4H_9)_4$ occurs quickly and produces $Ti(OH)_4$ precipitates when there was too much water around the precursor molecules. Fast hydrolysis does not favor the formation of porous structures because the precipitates impede the interaction of the precursor and soft templates.

Under the same post-extraction by nitric acid with the same concentration of 0.15 mol l^{-1}, and after TiO_2-1, TiO_2-3 and TiO_2-4 were processed by different ultrasonic energy sources, they gain different structures. There is no porous structure in TiO_2-3 that is prepared under the intensity of 100 W cm^{-2} ultrasound and at 298 K. However, TiO_2-1 has a porous structure. Although TiO_2-1 is synthesized under 50 W cm^{-2} intensity of ultrasound, its aging temperature is 333 K. Heat provides some energy that is required for the formation of porous structure. TiO_2-4 with porous structure is prepared under the intensity of 250 W cm^{-2} ultrasound, aged at 298 K. TiO_2-1 and TiO_2-4 have porous structures, which are synthesized under higher energy source. Ultrasound produces the localized hot spots through compression and shock wave formation within the gas phase of the collapsing bubble. The high temperature in the interface between gas phase and bulk solution can accelerate the condensation of titanium hydroxide, shorten the synthesis time and enhance the thermal stability of the precipitates [8]. Proper heating is needed for the formation of hydrogen bonding between the template alkylamine-H and the oxygen of precursor. The energy of the ultrasound can influence the formation of a mesoporous structure [9].

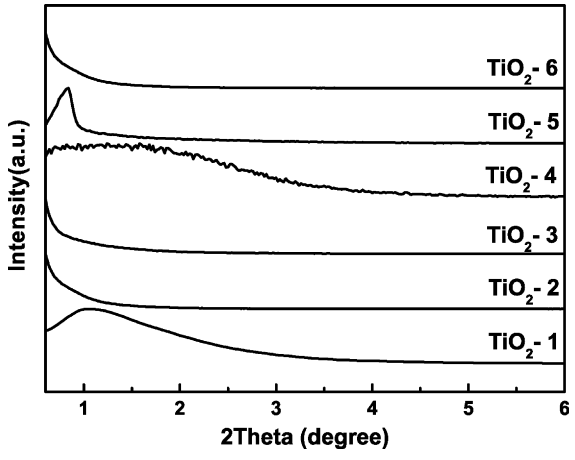

Fig. 2. Low-angle XRD pattern of TiO_2 calcined at 673 K for 4 h.

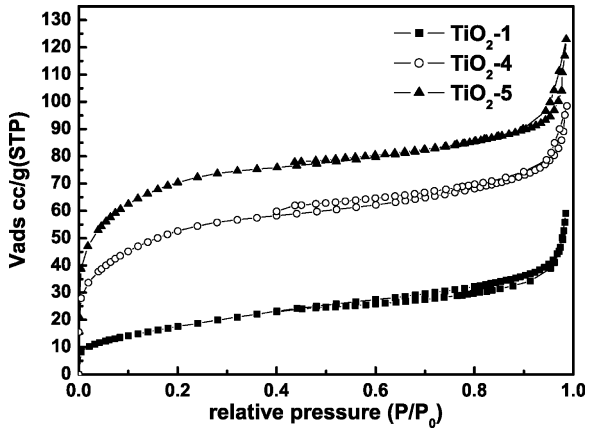

Fig. 3. N_2 adsorption–desorption isotherm curve of macro-mesoporous TiO_2.

In order to remove the templates from the pores, nitric acid is used to weaken the interaction between the template molecules and the inorganic precursor. TiO_2-4, TiO_2-5 and TiO_2-6 are prepared through the same ultrasonic energy and the same calcinations, but they are post-treated by nitric acid with different concentrations. There is no pore in TiO_2-6 post-treated with 0.015 mol l^{-1} nitric acid. However, TiO_2-4 and TiO_2-5 contain porous structures, which are processed by 0.15 and 1.5 mol l^{-1} nitric acid, respectively. The results show that nitric acid with lower concentration cannot remove the template molecules completely. Although TiO_2-4 and TiO_2-5 contain porous structures, they have poor crystallization. It is possible that higher concentration of nitric acid does not favor the crystallization of TiO_2.

3.2. N_2 adsorption–desorption isotherm

According to the results of low-angle XRD, TiO_2-1, TiO_2-4 and TiO_2-5 with one diffraction peak at low angle have porous structures. Fig. 3 shows the nitrogen adsorption and desorption isotherms for TiO_2-1, TiO_2-4 and TiO_2-5 with porous structure. From the shape of the adsorption–desorption isotherm curves, the types of pore can be estimated. Their isotherms are considered as a combination of type I and type IV because the isotherm exhibited high adsorption at low relative pressure, which indicates that there are micropores. However, at high relative pressure between 0.45 and 1.0, the curves exhibit a small hysteresis loop, indicating the presence of mesopores. The curve of TiO_2-1 belongs to type H3, which indicates that the porous structure is disorder. The curves of TiO_2-4 and TiO_2-5 are of type H4, which shows the pore structure is ordered. In a type IV isotherm, there is a small stepwise increase appearing at relative pressure 0.2, indicating capillary condensation in the mesopores. However, hysteresis loop does not appear at P/P_0 0.2. The hysteresis loop appearing at P/P_0 0.45 is attributed to

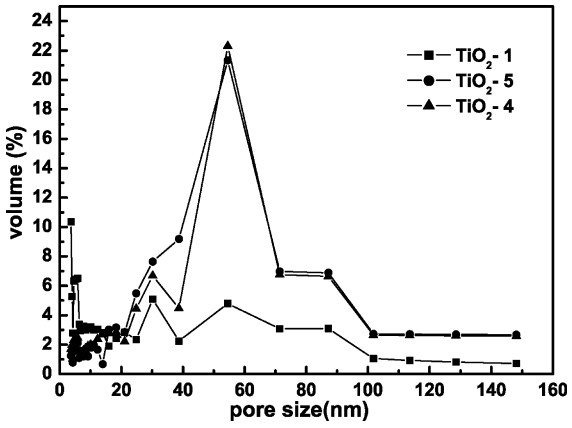

Fig. 4. Pore size distribution of TiO_2-1, TiO_2-4 and TiO_2-5.

the intergranular spacing between agglomerated particles. There is a small step at a relative pressure of 0.95 corresponding to the mesoporous adsorption [10]. The specific surface area of TiO_2-1, TiO_2-4 and TiO_2-5 is 93.09, 289.45 and 317.94 $m^2\,g^{-1}$ respectively, while the specific surface area of TiO_2-2, TiO_2-3 and TiO_2-6 is 110.39, 47.59 and 17.91 $m^2\,g^{-1}$. The BJH pore size curves obtained from the desorption branch of the isotherm are shown in Fig. 4, which indicate that TiO_2-4 and TiO_2-5 have relatively sharp pore size distribution (around 50 nm), while TiO_2-1 has a broad distribution of pore size from micropore to macropore. A wide distribution of size for TiO_2-1 may be attributed to the heat in the synthesis process. TiO_2-1 is prepared under ultrasound with an intensity of 50 W cm^{-2}, assisted by heat at a temperature 333 K, while TiO_2-4 and TiO_2-5 are synthesized under ultrasound with an intensity of 250 W cm^{-2}, aged at 298 K.

3.3. Photocatalytic activity

Anatase TiO_2 nanoparticles exhibit relatively high photocatalytic activity in the oxidation of organic pollutants [11–13]. In this study, the photocatalytic activity of the as-prepared TiO_2 samples was investigated by degrading toluene in UV light. Fig. 5 shows the results of photocatalytic activity of TiO_2 to oxidize toluene with an original concentration of 7.528 μmol l^{-1}. Before the UV light is turned on, it is found that the concentration of toluene decreases with equilibration time when TiO_2 exits in the quartz reactor. The concentrations of toluene are compared over different TiO_2 photocatalysts after equilibration for 120 min. The order of toluene concentration is as follows, $C_{TiO_2\text{-}6} > C_{TiO_2\text{-}3} > C_{TiO_2\text{-}2} > C_{TiO_2\text{-}1} > C_{TiO_2\text{-}4} > C_{TiO_2\text{-}5}$, which indicates that TiO_2 photocatalysts with porous structures and high specific surface areas can adsorb large amounts of toluene gas molecules on their surfaces. The concentrations of toluene over TiO_2-1, TiO_2-4 and TiO_2-5 are lower than those over TiO_2-2, TiO_2-3 and TiO_2-6, which imply that porous structures provide more interfaces for adsorption of toluene molecules. If there is no porous structure, TiO_2 with a higher specific surface area can absorb more toluene molecules. TiO_2-1 can absorb more toluene because it has a porous structure although TiO_2-2 has a higher specific surface area than TiO_2-1.

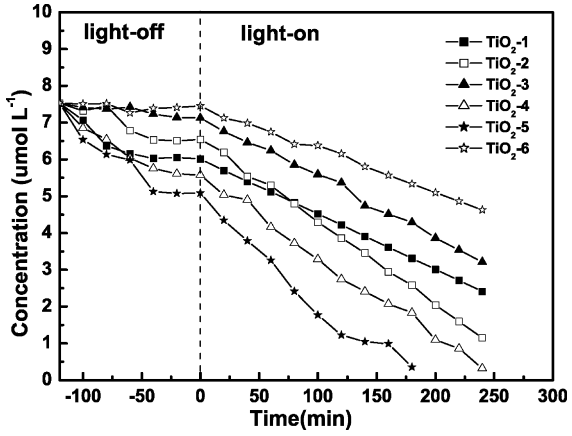

Fig. 5. Photocatalytic activity of TiO_2 calcined at 673 K for 4 h.

Under irradiation by UV light, the photocatalytic degradation process occurs on the interface of the adsorbed substrate and the adsorbed reactive species. With increasing irradiation time, the concentration of toluene decreases in the quartz reactor. Different photocatalytic degradation rate is gained with a different TiO_2 sample, which is shown in Fig. 5. Photocatalytic products of toluene over TiO_2 are phenylaldehyde and phenylformic acid that are intermediate products. The final products of photocatalytic degradation of toluene are CO_2 and H_2O [14].

In general, the diffusion rate of adsorbed reactive species on the surface is faster than the photocatalytic reaction rate. Therefore, the photocatalytic reaction is the rate control step. The photocatalytic degradation can be described with the Langmuir–Hinshelwood equation [15]:

$$R = \frac{k_{L\text{–}H} K C}{(1 + KC)},$$

where R is the reaction rate, $k_{L\text{-}H}$ the reaction rate constant, K the Langmuir adsorption constant, C the reactant concentration. When the concentration of reactant is sufficiently high, the photocatalytic reaction is of zero order. The rate has little dependence on the concentration of toluene. The dependence of toluene concentration on the irradiation time is linear. The rate constants of photocatalytic reaction over six TiO_2 samples are shown in Table 1. The order of rate constant of photocatalytic degradation is as follows: $k_{TiO_2\text{-}5} > k_{TiO_2\text{-}2} > k_{TiO_2\text{-}4} > k_{TiO_2\text{-}3} > k_{TiO_2\text{-}1} > k_{TiO_2\text{-}6}$. Pore structure and crystallization of TiO_2 can affect the rate of photocatalytic degradation of toluene. Although the crystallization of TiO_2-4 and TiO_2-5 is poor, they give higher rate constants for photocatalytic degradation of toluene because TiO_2-4 and TiO_2-5 contain porous structures that provide more active sites for photocatalytic reaction and facilitates the absorption of UV light onto photocatalyst surface. TiO_2-1, with a porous structure has a lower rate constant of photocatalytic degradation of toluene than TiO_2-2 and TiO_2-3 without porous structures, which may be attributed to the fact that some reactive sites of TiO_2-1 is unexposed or blocked by trace surfactant template. Crystallization is another fact that decides photocatalytic efficiency. However, active sites in the porous structure are more important than crystallization for improving the efficiency of photocatalytic degradation of toluene.

4. Conclusions

Porous TiO_2 was synthesized through a sonochemical approach followed by acid treatment for removing templates and calcination at 673 K for 4 h. Proper ultrasonic energy and heating facilitate the formation of pores. Nitric acid with lower concentration does not favor template removal and pore formation. The rate constant of photocatalytic degradation of toluene by as-prepared TiO_2 is compared as follows: $k_{TiO_2\text{-}5} > k_{TiO_2\text{-}2} > k_{TiO_2\text{-}4} > k_{TiO_2\text{-}3} > k_{TiO_2\text{-}1} > k_{TiO_2\text{-}6}$. The results show that TiO_2 with a porous structure and a high specific surface area exhibits superior photocatalytic properties, although they have poor crystallization.

Acknowledgements

This work was supported by the National Natural Science Foundation of China (Nos. 20221101, 10335040 and 20671004), Beijing Municipal Commission of Education Foundation (Grants No. KM 200311417141) and Beijing Foundation for Elitists (Grants No. 20051D0502208).

References

[1] L. Wu, J.C. Yu, X.C. Wang, L.Z. Zhang, Characterization of mesoporous nanocrystalline TiO_2 photocatalysts synthesized via a sol-solvothermal process at a low temperature, J. Solid State Chem. 178 (2005) 321.

[2] S. Rodrigues, K.T. Ranjit, Single-step synthesis of a highly active visible-light photocatalyst for oxidation of a common indoor air pollutant:Acetaldehyde, Adv. Mater. 17 (2005) 2467.

[3] Q. Dai, L.Y. Shi, Y.G. Luo, J.L. Blin, et al., Effects of templates on the structure, stability and photocatalytic activity of mesostructured TiO_2, J. Photochem. Photobiol., A 148 (2002) 295.

[4] H. Yoshitake, T. Sugihara, T. Tatsumi, Preparation of wormhole-like mesoporous TiO_2 with an extremely large surface area and stabilization of its surface by chemical vapor deposition, Chem. Mater. 14 (2002) 1023.

[5] S. Han, S.H. Choi, S.S. Kim, Low-temperature synthesis of highly crystalline TiO_2 nanocrystals and their application to photocatalysis, Small 1 (2005) 812.

[6] X.C. Wang, J.C. Yu, C. Ho, Y.D. Hou, et al., Photocatalytic activity of a hierarchically macro/mesoporous titania, Langmuir 21 (2005) 2552.

[7] B. Smarsly, D. Grosso, T. Brezesinski, et al., Highly crystalline cubic mesoporous TiO_2 with 10 nm pore diameter made with a new block copolymer template, Chem. Mater. 16 (2004) 2948.

[8] A. Corma, From microporous to mesoporosu molecular sieve materials and their use in catalysis, Chem. Rev. 97 (1997) 2373.

[9] K. Okitsu, M. Ashokkumar, F. Grieser, Sonochemical synthesis of gold nanoparticles: effects of ultrasound frequency, J. Phys. Chem. B 109 (2005) 20673.

[10] F. Jiao, P.G. Bruce, Two-and three-dimensional mesoporous iron oxide with microporous wall, Angew. Chem. Int. Ed. 43 (2004) 595.

[11] L.X. Cao, Z. Gao, S.L. Suib, et al., Photocatalytic oxidation of tolune on nanoscale TiO_2 catalysts: studies of deactivation and regeneration, J. Catal. 196 (2000) 253.

[12] P. Calza, C. Minero, A. Hiskia, et al., Photocatalytic transformation of CCl_3Br, CBr_3F, $CHCl_2Br$ and CH_2BrCl in aerobic and anaerobic conditions, Appl. Catal. B 29 (2001) 23.

[13] A. Sirisuk, C.G. Hill Jr., M.A. Anderson, et al., Photocatalytic degradation of ethylene over thin films of titania supported on glass rings, Catal. Today 54 (1999) 159.

[14] Y. Liu, Y. Li, et al., Study on photocatalytic degradation of indoor air VOCs: toluene over TiO_2 nanoparticles, Acta Sci.Circumstant. 26 (2006) 12.

[15] Y.M. Xu, C.H. Langford, Variation of Langmuir adsorption constant determined for TiO_2-photocatalyzed degradation of acetophenone under different light intensity, J. Photochem. Photobiol., A 133 (2000) 67.